Monte Carlo simulations of magnetron sputtering particle transport

A. M. Myers, J. R. Doyle, J. R. Abelson, and D. N. Ruzic

Citation: J. Vac. Sci. Technol. A 9, 614 (1991); doi: 10.1116/1.577375

View online: http://dx.doi.org/10.1116/1.577375

View Table of Contents: http://avspublications.org/resource/1/JVTAD6/v9/i3

Published by the AVS: Science & Technology of Materials, Interfaces, and Processing

Related Articles

The Si3N4/TiN Interface: 4. Si3N4/TiN(001) Grown with a −250 V Substrate Bias and Analyzed In situ using Angle-resolved X-ray Photoelectron Spectroscopy
Surf. Sci. Spectra 19, 62 (2012)

The Si3N4/TiN Interface: 1. TiN(001) Grown and Analyzed In situ using Angle-resolved X-ray Photoelectron Spectroscopy
Surf. Sci. Spectra 19, 33 (2012)

The Si3N4/TiN Interface: 5. TiN/Si3N4 Grown and Analyzed In situ using Angle-resolved X-ray Photoelectron Spectroscopy
Surf. Sci. Spectra 19, 72 (2012)

The Si3N4/TiN Interface: 6. Si/TiN(001) Grown and Analyzed In situ using Angle-resolved X-ray Photoelectron Spectroscopy
Surf. Sci. Spectra 19, 82 (2012)

The Si3N4/TiN Interface: 2. Si3N4/TiN(001) Grown with a −7 V Substrate Bias and Analyzed In situ using Angle-resolved X-ray Photoelectron Spectroscopy
Surf. Sci. Spectra 19, 42 (2012)

Additional information on J. Vac. Sci. Technol. A

Journal Homepage: http://avspublications.org/jvsta

Journal Information: http://avspublications.org/jvsta/about/about_the_journal

Top downloads: http://avspublications.org/jvsta/top_20_most_downloaded

Information for Authors: http://avspublications.org/jvsta/authors/information_for_contributors

ADVERTISEMENT

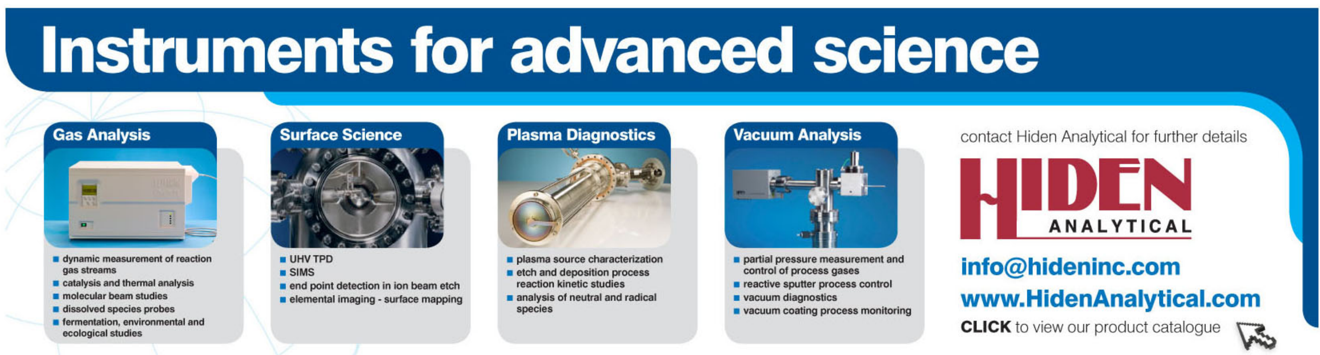

Downloaded 23 Dec 2012 to 192.17.144.173. Redistribution subject to AVS license or copyright; see http://avspublications.org/jvsta/about/rights_and_permissions

Monte Carlo simulations of magnetron sputtering particle transport

A. M. Myers,[a] J. R. Doyle, and J. R. Abelson[a]
Coordinated Science Laboratory, University of Illinois, 1101 W. Springfield, Urbana Illinois 61801

D. N. Ruzic
Department of Materials Science and Engineering, University of Illinois, Urbana, Illinois 61801

(Received 9 October 1990; accepted 26 November 1990)

Monte Carlo simulations of the particle transport process during dc magnetron sputter deposition were performed to determine the energy and angular distributions of the energetic deposition species. The model itself is quite general, and here we present the specific example of hydrogenated amorphous silicon film growth. This process involves the sputtering of a silicon target in an argon-plus-hydrogen plasma. The three-dimensional model incorporates fractal TRIM data for the distribution of Si energies and emission angles sputtered from the target surface. Modified "universal" interatomic potentials are used to determine the scattering processes during gas phase transport. Energy and angular distributions of the deposition flux reaching the substrate are calculated as a function of pressure from 0.01 to 5.5 mTorr. As the pressure increases we find that the average energy per deposited atom remains essentially constant, but the energy and angular distributions of the arrival flux change dramatically.

I. INTRODUCTION

Magnetron sputtering is used to deposit thin films in a variety of industrial and research applications. The final material properties are significantly influenced by the energies and angles at which species impact the growth surface. While the pressures used in dc magnetron sputtering are low (1–10 mTorr), a sputtered species may still undergo a significant amount of scattering before arriving onto the substrate surface. These collisional processes will affect both the energies and angles of the coating flux.

There has been a great deal of research detailing the effects of gas pressure, substrate temperature, and energetic bombardment on a film's microstructural properties, and excellent reviews have been published by Messier *et al.*,[1] Harper,[2] and Greene.[3] Yehoda *et al.*[4] studied microstructural densification as a function of the energy input into the growing surface, while Thornton[5] studied the effects of arriving angle on film microstructure. These effects are unified in the structure zone model (SZM) of Thornton[6] and Messier *et al.*[7] It shows that the microstructure changes from low-density columnar grains to a dense fine grained structure as the pressure decreases. Bombardment induced mobility is also critical in determining the material microstructure. All these studies underscore the critical need to know the energy and angular distributions of the arrival flux in thin film deposition.

In the present study, we were motivated to understand the growth of hydrogenated amorphous silicon (*a*-Si:H) thin films. This material has important technological applications in photovoltaics, thin-film transistors and xerography. The two most common deposition techniques for *a*-Si:H are plasma-assisted chemical vapor deposition (PACVD), i.e., the decomposition of silane in a glow discharge, and reactive sputtering (RS), where a silicon target is sputtered in an argon-plus-hydrogen plasma. Recent measurements of *a*-Si:H RS using a 2 in. magnetron source have confirmed that the coating flux is $\sim 10\%$ SiH and $\sim 90\%$ Si.[8] These are very reactive species, expected to have high sticking coefficients and low surface mobilities. The growth appears to be dominated by physical vapor deposition processes in which the energy and angular distributions of the arriving flux are crucial to film quality.

The magnetron sputtering deposition flux has been modeled in several Monte Carlo studies, which have been reviewed by Turner *et al.*[9] Most of the past work either used simplified gas scattering models (e.g., hard spheres), impractical deposition geometries (e.g., infinite parallel planes), or analytical approximations to the energy and angular distributions of nascent sputtered particles. The present study overcomes all these limitations, and the results reported here are the most realistic yet achieved for magnetron sputter deposition. The emphasis in this report is on the pressure dependence of the angular and energy distribution of the arriving Si flux in the deposition of *a*-Si:H.

II. EXPERIMENTAL

The chamber geometry is shown in Fig. 1. Sputtering occurs in the racetrack of a 2 in. diam circular silicon target. An actual racetrack groove has been measured; in the model, the probability of particle ejection is weighted proportional to the depth of the groove. For the present simulations, a new, flat target was used. The target-to-substrate distance was kept constant at 8 cm, the chamber width was fixed at 20 cm, and the substrate was a square of side 2.54 cm centered over the target. Simulations as a function of chamber width showed that the results were relatively insensitive to this dimension, as long as the width was greater than the target-to-substrate distance. Theta (θ) describes the angle at which a particle arrives at the substrate with respect to the substrate normal. The argon pressure was varied between 0.01 and 5.5 mTorr. Addition of 0.5 mTorr H_2 to 1.5 mTorr Ar (typical

 0734-2101/91/030614-05$01.00 © 1991 American Vacuum Society

Downloaded 23 Dec 2012 to 192.17.144.173. Redistribution subject to AVS license or copyright; see http://avspublications.org/jvsta/about/rights_and_permissions

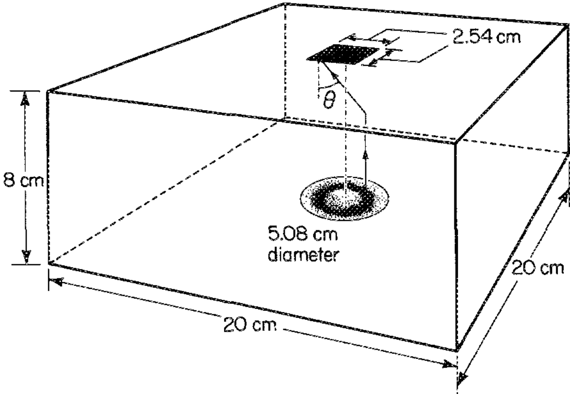

FIG. 1. Deposition geometry used for these simulations. Theta (θ) represents the angle of arrival of a particle with respect to the substrate normal. The relative dot density indicates the ejection probability from the target surface.

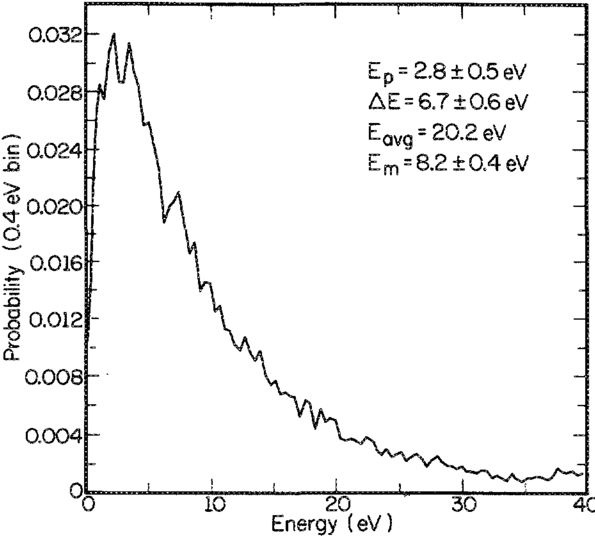

FIG. 2. Energy distribution of the nascent sputtered particles calculated by fractal TRIM. The probabilities were determined by dividing the energy spectra into 0.4 eV wide bins. Here E_p is the most probable energy, ΔE is the effective width of the distribution at half of the maximum probability, E_{avg} is the average energy, and E_m is the median energy.

a-Si:H growth pressures) did not affect the simulation results appreciably.

Fractal TRIM[10,11] was used to obtain the ejection angles and energies of the nascent sputtered particles. This method was chosen because analytical energy distributions generally assume a cosine angular distribution, with no angular dependence on energy. Fractal TRIM utilizes concepts from fractal geometry to simulate the atomic scale roughness that exists in the first few atomic layers of a surface undergoing bombardment. The independent inputs to the fractal TRIM code are surface binding energy, fractal surface dimension, which is a measure of surface roughness, and the incident ion energy. A binding energy of 5.1 eV and a fractal surface dimension d of 2.01 was found to give the best fit to measured sputter yields[12] over the range 0.1–1 keV. This dimensionality corresponds to a ± 4 Å variation in the surface topography over an 80 Å surface length. Differences between fractal TRIM and standard planar TRIM occur only at low ion energies or at grazing ion incidence angles. Thus the use of fractal versus planar TRIM is not expected to significantly affect the results reported here.

Ideally, an actual ion energy distribution such as the one calculated by Goeckner *et al.*[13] should be used to launch the sputtered ions in the fractal TRIM code. For the current model, however, the distribution in Ref. 14 was weighted with experimental sputter yield data and calculated an average effective incident ion energy was calculated; this was found to be 365 eV for a 450 V cathode voltage (a typical voltage for *a*-Si:H deposition). The energy distribution of the nascent sputtered particles coming off the target under these conditions is shown in Fig. 2. For this simulation a data set of 24 091 ejected particles was used. Varying the size of the fractal TRIM data set from 8227 to 24 091 launches decreased the noise in the distribution data, but had no other effect on the simulation results. The fractal TRIM results showed that 143 argon atoms were reflected from the target surface. Since this was only 0.6% of the sputtered flux, the effects of these reflected Ar atoms were ignored.

After ejection from the target, a sputtered Si atom may undergo a number of scattering events with background Ar atoms before striking the substrate surface. To describe this interaction the "universal" interatomic potential was used.[14] Because this potential is accurate only for scattering events with energies greater than approximately 2 eV, it was modified to incorporate a r^{-6} van der Waals attractive well at low energies. Using this potential, reference tables of scattering angle versus impact parameter were generated for energies up to 365 eV. The energy-dependent total cross section was defined as $\pi(b_{\max})^2$, where $b_{\max}$ is the impact parameter that results in a deflection angle of less than 1° in the center-of-mass frame. Free paths and impact parameters were selected using standard Monte Carlo techniques. The argon background gas was taken to be at room temperature. Rossnagel has shown that significant background gas rarefaction will occur at high cathode current densities, with high gas pressures and long target-to-substrate distances.[15] However, for the conditions used in this simulation, the current density is low (22 mA/cm^2, based on our standard experimental conditions), and most of the sputtered particle energy is deposited into the chamber walls and substrate rather than the gas. Therefore the gas density will not be significantly reduced.

In our treatment of the scattering process, the background argon gas is assumed to have negligible velocity. Thus our method cannot be applied to collision events where the Si atom energies are comparable to those of the room temperature background gas, and a sputtered particle cannot be followed to arbitrarily low translational energy. It was assumed that the energy at which particle tracking was no longer valid occurred at 0.26 eV (one order of magnitude above thermal); all particles whose energies were lower were denoted "quasithermalized." If a particle became quasithermalized, its location was noted and a new particle was launched. A given particle's trajectory was followed until it either struck

Downloaded 23 Dec 2012 to 192.17.144.173. Redistribution subject to AVS license or copyright; see http://avspublications.org/jvsta/about/rights_and_permissions

the substrate, the chamber wall, or became "quasithermalized."

All simulations were performed on a Cray X-MP supercomputer. The depositions were run until 25 000 Si atoms arrived at the substrate. As the pressure was increased from 0.01 to 4.5 mTorr of argon, the number of sputtering events increased from 1.7×10^6 to 2.3×10^6, the total number of scattering events increased from 3.0×10^4 to 1.9×10^7, and the simulation time increased from 96 to 753 cpu seconds.

III. RESULTS AND DISCUSSION

The probability that a sputtered Si atom will arrive at the substrate with a particular energy above 0.26 eV is shown in Figs. 3(a)–3(c). The contribution of quasithermal particles will be discussed below. The probabilities were determined by dividing the total arrival flux into bins 0.4 eV wide. A qualitative change in the shape of the curves, including a shift to lower energies, is observed as the pressure is increased from 0.5 to 4.5 mTorr. Note that the average energy per deposited atom, E_{avg}, remains almost unchanged. This constancy in E_{avg} is apparently the result of the energy-dependent cross sections used in our model. On the one hand, increasing the argon pressure results in more scattering for the arriving Si atoms during transit from the target to substrate, tending to lower their average energy. On the other hand, particles ejected at low energy scatter more frequently and on average at higher angles (higher angle scattering results in greater energy transfer), removing them from the substrate-directed flux and/or quasithermalizing them. In the average energy calculation, where higher energy particles are weighted more than lower energy ones, these effects apparently compensate. We checked this interpretation by running simulations with energy-independent hard-sphere cross sections for gas phase scattering, and the same nascent sputter distribution from fractal TRIM. These simulations result in a large drop in E_{avg}, from 10.84 to 6.01 eV over the same pressure range, as predicted.

When the nascent particles have a distribution of energies, the pressure dependence of the average energy per deposited species is not necessarily a useful parameter to correlate with material properties. However, the simulation results [Figs. 3(a)–3(c)], indicate that the median energy, the most probable energy and its probability, and the energy width of the distribution, are all sensitive to pressure. With increasing Ar pressure, the median energy E_m decreases, while the maximum probability increases and its location E_p decreases. The distributions also become much narrower with increasing pressure. These results show that indeed the bulk of the energetic particles arriving at the substrate will have a lower energy as the pressure is raised. The noise in the low pressure curves is a consequence of the limited number of Monte Carlo fractal TRIM events. At higher pressures, enough scattering has taken place to smooth out the distribution.

Also shown in Figs. 3(a)–3(c) are the energy distributions of those particles arriving at angles to the substrate normal between 0° and 30°, 30° and 60°, and 60° and 90°, as well as the distribution of those particles that have not undergone a scattering event with the background gas. In our system geometry, an unscattered particle can arrive at the

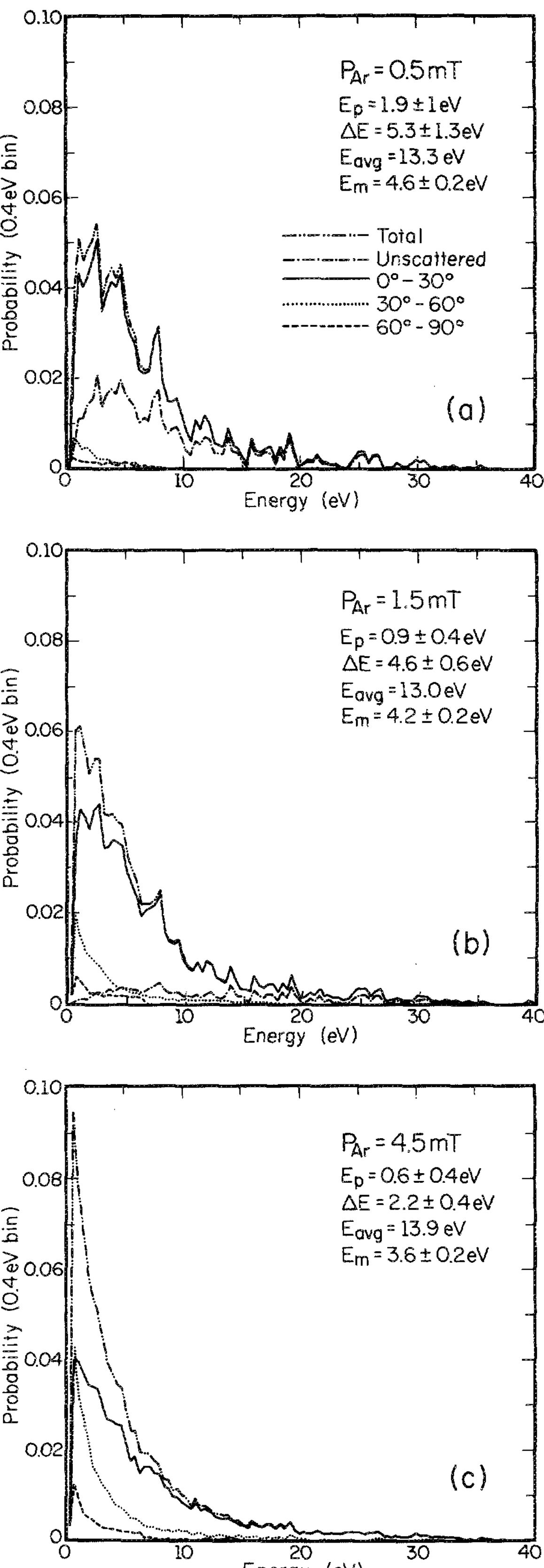

FIG. 3. The energy distribution of the depositing Si atoms for Ar pressures of 0.5, 1.5, and 4.5 mTorr. The probabilities were determined by dividing the energy distribution into 0.4 eV wide bins. Shown are the total arrival distribution, the distribution of those particles that did not undergo a scattering event, and the distributions of particles arriving with θ between 0° and 30°, 30° and 60°, and 60° and 90°. The distribution parameters are defined in Fig. 2.

Downloaded 23 Dec 2012 to 192.17.144.173. Redistribution subject to AVS license or copyright; see http://avspublications.org/jvsta/about/rights_and_permissions

substrate with theta (θ) no larger than 25.7°. At 0.5 mTorr, the distribution is dominated by particles arriving at "line-of-sight" angles to the substrate. While Fig. 3(a) shows that over half of the deposition flux has undergone a scattering event (consistent with the average mean-free path at this pressure and the target–substrate distance), most of these collisions resulted in low-angle deflections. Those particles that arrive at larger angles have suffered enough collisions and/or have scattered through large angles to appreciably degrade in energy, which significantly shifts their distributions to lower energies. The distribution at 1.5 mTorr shows that the line-of-sight component is becoming smaller. Also, the energy filter effect can be seen in the small unscattered distribution curve. Since the lower-energy particles are preferentially scattered, the low-energy portion of the unscattered distribution has decreased faster than the high-energy portion. At 4.5 mTorr we see that the contribution of the large-angle deposition flux has increased dramatically and the unscattered flux has disappeared.

Geometric effects also play a role in determining the depositing species' energy distributions since the nascent sputtered particles are not angularly isotropic with energy. From the fractal TRIM calculation, the average energy at which a silicon atom is sputtered from the target increases with the emission angle. For the unscattered particles, and those particles that have undergone small-angle scatterings, the small substrate area (6.45 cm^2) mainly intersects the lower-energy portion of the sputtered flux. Keeping in mind the above caveats on average energy, we note that the sputtered particles have an average energy of 20.24 eV, while E_{avg} of the arrival species is approximately 13.5 eV. However, when the size of the substrate is increased to the chamber width (approximating an infinite parallel plate geometry), we find the average energy of arrival to be 19 eV. This confirms the importance of using realistic geometry and sputter distributions for these kinds of simulations.

The probability that an energetic sputtered Si atom will arrive at a particular angle with respect to the substrate is shown in Figs. 4(a)–4(c). These probabilities were determined by dividing the total arriving flux into 1° wide bins. Also shown on these figures is the angular distribution of energetic particles that have undergone 0, 1, 2, 3, or more scattering events. Thus at low pressure, the angular distribution is peaked below 25.7° and only a small high-angle tail is observed on the distribution. This tail is due to the few large-angle collisions that scatter particles onto the substrate that were not ejected at line-of-sight angles. At 1.5 mTorr, the number of arriving particles that have undergone several and/or large-angle collisions has become significant, resulting in a larger high-angle tail on the distribution. At 4.5 mTorr, deposition is dominated by the more highly scattered flux, although the distribution still peaks at line-of-sight angles. Over this pressure range, the average angle of arrival of a deposited species nearly doubles, going from 12.7° to 24°.

The possible contribution of thermal or quasithermal particles to the deposition process should be considered. Figure 5 shows the fraction of the total sputtering events that become quasithermalized. At the typical deposition pressure of 1.5 mTorr Ar, we find that only 5.3% of the total sputtered

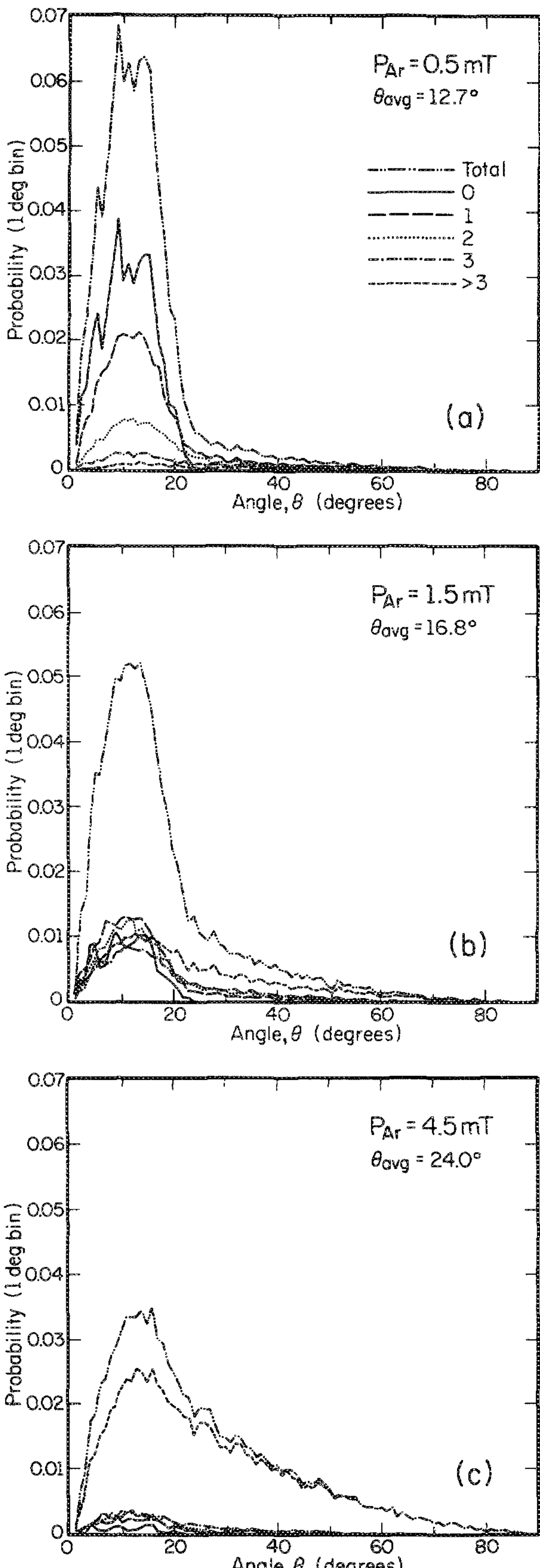

FIG. 4. The angular distribution of the depositing Si atoms for Ar pressures of 0.5, 1.5, and 4.5 mTorr. The probabilities were determined by dividing the angular distribution into 1° bins. Shown are the total arrival distribution and the distributions for particles that have undergone 0, 1, 2, 3, or greater than 3 scattering events. Here θ_{avg} is the average angle of arrival of a depositing species.

Downloaded 23 Dec 2012 to 192.17.144.173. Redistribution subject to AVS license or copyright; see http://avspublications.org/jvsta/about/rights_and_permissions

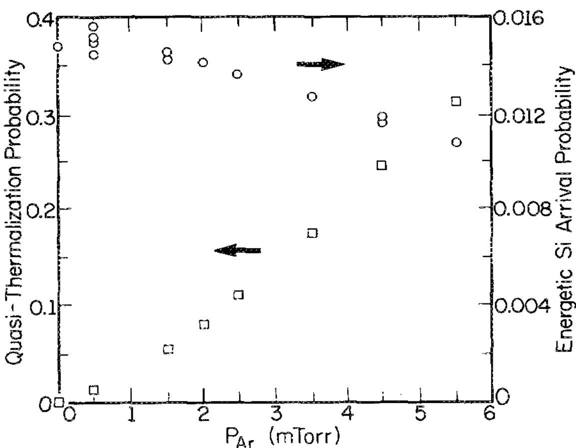

FIG. 5. The probability that a sputtered particle will become quasithermalized before depositing on the substrate or being lost from the chamber vs pressure. Also shown is the probability that a sputtered Si atom will arrive at the substrate before being lost from the chamber or quasithermalized.

material becomes quasithermal. However, at 5.5 mTorr, 31% of the sputtered flux has fallen below 0.26 eV. Consequently, at these high pressures the quasithermals could be making a significant contribution to growth. Their spatial distribution is peaked near the sputtering target because the low-energy sputtered particles, which have large scattering cross sections, produce most of the quasithermal population.

To roughly estimate the quasithermal contribution to film growth, we consider the quasithermalization locations as isotropic point sources of Si atoms, and divided the chamber into 900 cubes. The number of quasithermals arriving at the substrate from any given cube is taken as the fraction of the total solid angle subtended by the substrate at the center of the cube multiplied by the number of quasithermals within the cube. These contributions are then summed over the entire quasithermal spatial distribution. This simple model neglects diffusional and boundary effects, and also ignores the directed motion of the quasithermals toward the substrate plane. However, the former simplification will lead to an overestimation in the quasithermal deposition flux, while the latter will underestimate it, and these effects will tend to cancel out. The model shows that at the typical *a*-Si:H deposition pressure of 1.5 mTorr, only 4.0% of the depositing flux is due to these low-energy particles. While this is only a rough estimate, it is likely that at this pressure the thermals are not making a significant contribution to the total deposited flux. Also shown in Fig. 5 is the probability that an energetic sputtered particle arrives at the substrate surface. While the energetic arrival probability does decrease with increasing pressure, the change is small, decreasing only 28% as the pressure goes from 0.5 to 5.5 mTorr.

IV. CONCLUSIONS

We have presented detailed energy and angular distributions of the silicon atom arrival flux during magnetron sputter deposition of *a*-Si:H using fractal TRIM sputter distributions and Monte Carlo simulation of gas phase scattering with realistic potentials. These distributions were found to be strongly dependent on the background gas pressure, as expected. However, the average energy per deposited atom was not found to be a sensitive parameter and complete details of the distribution must be considered. A simplified calculation indicates that the low-energy "quasithermalized" component of the sputtered atoms does not contribute appreciably to deposition at typical *a*-Si:H deposition pressures.

ACKNOWLEDGMENTS

The authors wish to thank Dr. Ivan Petrov for many helpful discussions. We also thank Dr. W. Eckstien and the Institüt für Plasmaphysik, Garching, Germany, for permission to use and alter the TRIM computer code. This work was funded by IBM, the Strategic User Program of the NSF National Center for Supercomputing Applications at the University of Illinois, and the Electric Power Research Institute under Contract No. RP28241.

[a] Also at the Department of Materials Science and Engineering.

[1] R. Messier, J. E. Yehoda, and L. J. Pilione, in *Handbook of Plasma Processing Technology*, edited by S. M. Rossnagel, J. J. Cuomo, and W. D. Westwood (Noyes, New Jersey, 1990), Chap. 19, pp. 448–465.
[2] J. M. E. Harper, Solid State Technol. **30**, 129 (1987).
[3] J. E. Greene, Solid State Technol. **30**, 115 (1987).
[4] J. E. Yehoda, B. Yang, K. Vedam, and R. Messier, J. Vac. Sci. Technol. A **6**, 1631 (1988).
[5] J. A. Thornton, J. Vac. Sci. Technol. A **4**, 3059 (1986).
[6] J. A. Thornton, Annu. Rev. Mater. Sci. **7**, 239 (1977).
[7] R. Messier, A. P. Giri, and R. A. Roy, J. Vac. Sci. Technol. A **2**, 500 (1984).
[8] A. M. Myers, D. N. Ruzic, N. Maley, J. R. Doyle, and J. R. Abelson, *Amorphous Silicon Technology-1990*, edited by P. C. Taylor, P. G. LeComber, Y. Hamakawa, and A. Madan (Mat. Res. Soc, Pittsburgh, 1990), p. 595.
[9] G. M. Turner, I. S. Falconer, B. W. James, and D. R. Mckenzie, J. Appl. Phys. **65**, 3671 (1990).
[10] D. N. Ruzic and H. K. Chiu, J. Nucl. Mater. **162-164**, 904 (1989).
[11] D. N. Ruzic, Nucl. Instrum. Methods Phys. Res. B **47**, 118 (1990).
[12] D. N. Ruzic, in Handbook of Plasma Processing Technology, edited by S. M. Rossnagel, J. J. Cuomo, and W. D. Westwood (Noyes, Park Ridge, New Jersey, 1990), Chap. 19.
[13] M. J. Goekner, J. Goree, and T. E. Sheridan, IEEE Trans. Plasma Sci. (in press).
[14] J. F. Ziegler, J. P. Biersack, and U. Littmark, *The Stopping and Range of Ions in Solids*, edited by J. F. Ziegler (Pergamon, New York, 1985), Vol. I, pp. 24–48.
[15] S. M. Rossnagel, J. Vac. Sci. Technol. A**6**, 19 (1988).

Downloaded 23 Dec 2012 to 192.17.144.173. Redistribution subject to AVS license or copyright; see http://avspublications.org/jvsta/about/rights_and_permissions